A New East Asian Winter Monsoon Index and Associated Characteristics of the Winter Monsoon

JONG-GHAP JHUN AND EUN-JEONG LEE

School of Earth and Environmental Sciences, Seoul National University, Seoul, South Korea

(Manuscript received 27 September 2002, in final form 30 January 2003)

ABSTRACT

A new East Asian winter monsoon index, which reflects the 300-hPa meridional wind shear associated with the jet stream, was defined to describe the variability of the winter monsoon in midlatitude East Asia. This index represents very well the seasonal mean winter temperature over Korea, Japan, and eastern China. The National Centers for Environmental Prediction–National Center for Atmospheric Research reanalysis data from 1958 to 2001 were used to examine the composite structures of strong and weak winter monsoons based on this index. The composite strong winter monsoon is characterized by an enhanced upper-level jet stream south of Japan, a strengthened midtropospheric East Asian trough, a stronger than normal Aleutian low and Siberian high, and increased low-level northeasterlies along the Russian coast. This composite structure suggests that a cold winter in Korea and Japan depends critically on processes that control the pressure gradients between the Aleutian low and the Siberian high. Power spectral analysis of the index shows significant peaks occurring in 3–4, 6–8, and around 18 yr. The decadal peak is primarily due to a prominent cold period from 1980 to 1986 versus a warm period from 1987 to 1993. The regressed sea level pressure field for the interannual component resembles the composite strong winter monsoon pattern, whereas the sea level pressure pattern for the decadal component bears close similarity to that of the Arctic Oscillation. These conditions in the winter monsoon are associated with excess snowfall in October over the Siberian high, northeastern China, and far eastern Russia. The sensitivity experiments with the Seoul National University general circulation model suggest that the change in snow depth in autumn over the Siberian high and northeastern China may lead to the variability of the winter monsoon intensity. The teleconnection analysis confirms that development of the Siberian high and/or the Aleutian low is associated with an enhanced East Asian winter monsoon; the Arctic Oscillation is closely related to the winter monsoon intensity on the decadal time scale.

1. Introduction

There have been many efforts to understand the winter climate, and to predict the variation of the winter monsoon circulation in East Asia (Chang and Lau 1982; Chang et al. 1979; Ding and Krishnamurti 1987; Murakami 1987; Zhang et al. 1997). Zhang et al. (1997) summarized the mean winter monsoon circulation of East Asia. Their study indicated that the key driving force for the winter monsoon is the available potential energy generated by the differential heating between land and sea. The main heating source exists near the equatorial western Pacific. The latent heat release associated with intense convective precipitation in the equatorial western Pacific induces the local Hadley circulation in the meridional direction. To the far north of this convective center, a very strong cold dome lies near the Siberian region. The East Asian jet, the Siberian high, the 500-hPa trough, and the convection center near the western Pacific are inherently related to each other. These planetary-scale features characterize the three-dimensional winter monsoon circulation. Some previous studies showed the genesis and development of the Siberian high resulted from the combined effects of the mass convergence at middle and upper levels, and the radiative cooling (Ding and Krishnamurti 1987; Ding 1990). Ding and Krishnamurti (1987) illustrated that the intensity of the Siberian cold dome is maintained by the strong radiative cooling, the large-scale descending motion by the Siberian high, a strong local Hadley circulation, and the persistent cold-air advection throughout the troposphere. According to Murakami (1987), the Tibetan Plateau not only largely controls the flow configuration in the lower troposphere but also greatly influences the thermally driven direct Hadley cell and the 200-hPa jet stream.

Among the factors influencing the East Asian winter monsoon, the snow cover over the Eurasian continent may be used as a precursor of the winter climate variation in East Asia. Watanabe and Nitta (1999) showed that the decrease of snow cover of East Asia in autumn results in an increase in surface temperature in East

Corresponding author address: Prof. Jong-Ghap Jhun, School of Earth and Environmental Sciences, Seoul National University, Seoul 151-742, South Korea.
E-mail: jgjhun@plaza.snu.ac.kr

Asia, a decrease in sea level pressure and geopotential height at 500 hPa in the Arctic region, and an increase in sea level pressure and geopotential height at 500 hPa in the North Pacific. The results of Watanabe and Nitta (1999) also support those of Yamazaki (1989), which suggests that the decrease of the albedo in East Asia is associated with a weakening of the Aleutian low. Results from several atmospheric general circulation models (AGCMs) are quite consistent with the observation analysis (Walland and Simmonds 1997; Walsh and Ross 1988). Walsh and Ross (1988) ran the National Center for Atmospheric Research (NCAR) Community Climate Model version 0B (CCM0B) forecast model for 30 days for the cases of both extensive and reduced Eurasian snow cover in winter. The differences between the two model runs included a deeper Aleutian low and reduced air temperature throughout the lower half of the troposphere in the region over and downstream of the snow anomaly when the snow cover was more extensive. Walland and Simmonds (1997) also showed the effects of snow cover using an AGCM, and their results supported the previous results. For short- to medium-range weather forecasting, observational analyses also demonstrate the simultaneous relationship between the snow cover in East Asia and the atmospheric circulation downstream in winter, which is remarkably similar to that identified in those model runs. The positive snow cover anomaly over East Asia in midwinter is associated with a decrease in air temperature over this transient snow region, a stronger East Asian jet, and negative geopotential height anomalies at the 500-hPa level over the North Pacific Ocean (Clark and Serreze 2000).

The active and inactive northeasterly East Asian monsoons not only control the local weather and climate in the East Asian region but also exert a strong impact on the extratropical and tropical planetary-scale circulations (Chang and Lau 1982), and even influence the convection and the sea surface temperatures (SSTs) near the Maritime Continent (Chang et al. 1979). Zhang et al. (1996, 1997) found that the East Asian winter monsoon tends to be weaker during the mature phase of El Niño. There is a close relationship between ENSO and the interannual variation of the winter monsoon and the cold surge in East China (Zhang et al. 1997). Wang et al. (2000) recently noted the existence of a Pacific–East Asia teleconnection pattern with anticyclone (cyclone) anomalies emanating from the equatorial central Pacific northwestward toward East Asia during an El Niño (La Niña) winter. They further suggested that a positive thermodynamic feedback between the anticyclonic anomaly and the SST in the western North Pacific is responsible for the existence of this teleconnection. Kitoh's (1988) results imply potential impacts of the SST in the western North Pacific on the East Asian winter climate.

Many researchers are interested in the relationship between the Arctic Oscillation (AO) and global climate variation, including the East Asian monsoon. Gong et al. (2001) showed that the winter temperature over eastern China is strongly connected to the sea level pressure (SLP) variation in the high latitude of the Eurasian continent (Siberian high region). According to Gong et al., the positive phase of the AO is associated with the lower SLP over the polar region and much of the Eurasian continent. Therefore, the Siberian high may play an important role in connecting the AO and the surface temperature over eastern China. Gong et al. (2001) also suggested that the Eurasian pattern (EU) and the AO pattern might play more notable roles in the East Asian winter monsoon and the regional climate than the western Pacific pattern (WP). It has been found that the AO is strongly coupled to surface air temperature fluctuations over the Eurasian continent (Thompson and Wallace 2000a,b; Kerr 1999). The variability of some regional circulation systems such as the Aleutian low also shows an apparent relation to the AO (Overland et al. 1999). Thompson and Wallace (2000a) indicated that the temperature advection associated with the AO-related zonal component of the anomalous flow plays an important role in establishing and maintaining the stationary wave pattern.

In spite of the diverse efforts to explain the East Asian winter monsoon, many unexplained features and characteristics of the winter monsoon still remain. First of all, there are few defined indices for the winter monsoon, especially in midlatitude East Asia. In the case of the south East Asian and Indian summer monsoons, many meteorologists have defined the monsoon indices to investigate the characteristics of the summer monsoon (Lau et al. 2000; Wang and Fan 1999; Webster and Yang 1992). Therefore, our study tries to define a new East Asian winter monsoon index (EAWMI). It should be noted that the region of the East Asian winter monsoon in our study covers the area of northeastern China, Korea, and Japan, unlike the region used in most previous East Asian monsoon studies. Second, after Mantua et al.'s (1997) study, the decadal variation in the atmosphere and the ocean is one of the most interesting issues, but that in the East Asian winter monsoon is of relatively little concern as yet. To understand well the characteristics of the winter monsoon, the separation of interannual and interdecadal monsoon variabilities in East Asia is needed. Therefore, we will analyze the decadal characteristics of the East Asian winter monsoon using the EAWMI. Finally, the relationship between the East Asian winter monsoon and the global circulation is also needed to understand the monsoon system in more detail, though some previous studies revealed the relations both between ENSO and the midlatitude circulation and between the AO and the east China climate.

The datasets and model experiments used in our study are described in section 2. The definition of the EAWMI and its characteristics are presented in section 3. The effect of snow cover in autumn on the East Asian winter monsoon and the teleconnection of the East Asian monsoon are shown in section 4 and section 5, respectively.

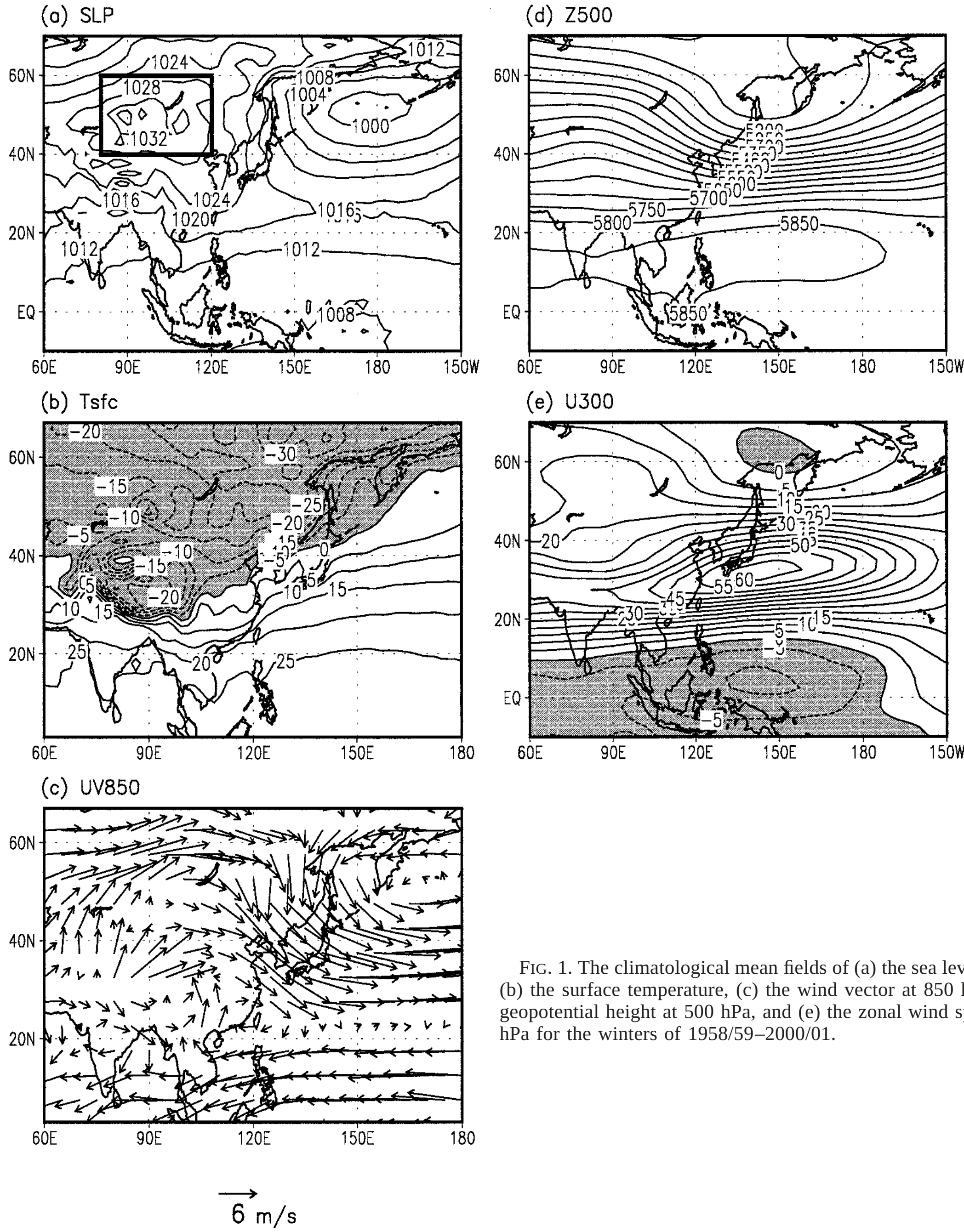

FIG. 1. The climatological mean fields of (a) the sea level pressure, (b) the surface temperature, (c) the wind vector at 850 hPa, (d) the geopotential height at 500 hPa, and (e) the zonal wind speed at 300 hPa for the winters of 1958/59–2000/01.

The summary and discussion are given in section 6 and section 7, respectively.

2. Data and model description

The observed data used in this study are obtained from the monthly mean reanalysis dataset of the National Centers for Environmental Prediction–National Center for Atmospheric Research (NCEP–NCAR) and the National Oceanic and Atmospheric Administration (NOAA) SST dataset for the 43-winter period from 1958/59 to 2000/01 (Kalnay et al. 1996). The resolution of the NCEP–NCAR reanalysis data is 2.5° in latitude and longitude along with the 12 pressure levels from 1000 to 100 hPa. The observed SST data from 1958/59 to 2000/01 are those reconstructed at NCEP. They have been obtained by applying a new interpolation method, based on spatial patterns from empirical orthogonal functions (EOFs) of SST anomalies for the period 1982–2001 to the monthly SST values of the Comprehensive Ocean–Atmosphere Data Set (COADS) for the period 1950–2001. The reconstructed SST fields

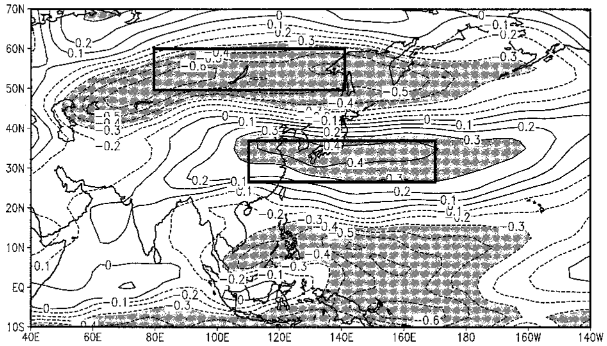

FIG. 2. The map of the correlation coefficient between the sea level pressure averaged over the boxed area of Fig. 1a and the zonal wind speed at each grid point at the 300-hPa level. The regions exceeding the 95% significance level are shaded.

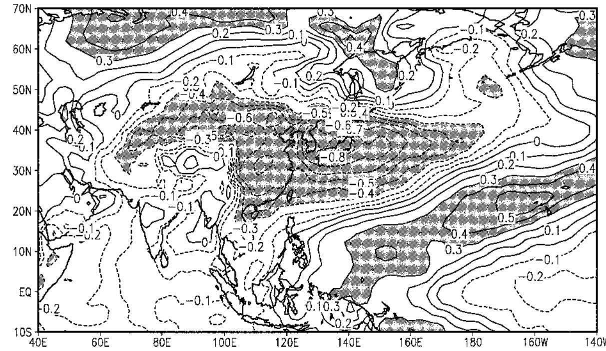

FIG. 4. The map of the correlation coefficient between the EAWMI and the surface temperature at each grid point. The regions exceeding the 95% significance level are shaded.

have lower root-mean-square differences than SST fields derived from the traditional NCEP–NCAR analysis of optimum interpolation. The horizontal resolution of SST data is 2° in latitude and longitude. Each winter season consists of the 3-month period from December to February. The snow cover data are derived from NOAA satellites and compiled at the National Environmental Satellite, Data, and Information Service. The data consist of weekly snow cover data, which indicate only the presence or the absence of snow in the Northern Hemisphere. The original 89 × 89 grid data spaced on a polar stereographic projection are converted to 180 × 45 grid data with a 2° × 2° resolution from December 1973 to February 2001. The snow depth data, which are used as an initial condition of the model experiment, are Atmospheric Model Intercomparison Project (AMIP) climatological data.

The Seoul National University (SNU) AGCM (SNU-AGCM), with triangular truncation at the two-dimensional wavenumber 31 (T31), which has been developed in the Climatological Dynamics Laboratory of SNU, is used in our computations. This spectral model is based on the three-dimensional primitive equations with 20 vertical levels. The SNU-AGCM consists of several physical processes and a detailed explanation of the model is provided by Kim (1999).

3. Structures of strong and weak monsoons

a. Definition of the East Asian winter monsoon index

As mentioned above, the climate in the East Asian region is greatly influenced by the monsoon circulation, and many studies have shown that the Siberian high is important for forming the monsoon circulation in the wintertime. In order to describe the intensity of the winter monsoon circulation, we define the East Asian winter monsoon index (EAWMI) in our study. Before defining the EAWMI, the climatological mean fields for the winters of 1958/59–2000/01 are summarized (Fig. 1). These climatological mean fields are characterized by the Siberian high and the Aleutian low in the sea level pressure system, the significant meridional temperature gradient of surface temperature in the East Asian region, the predominant northwesterlies over northeastern Asia in the lowest troposphere, the strong trough over northeastern Asia at 500 hPa, and the strong polar jet stream just south of Japan at 300 hPa. The central area of the Siberian high, which is located in the region 40°–60°N,

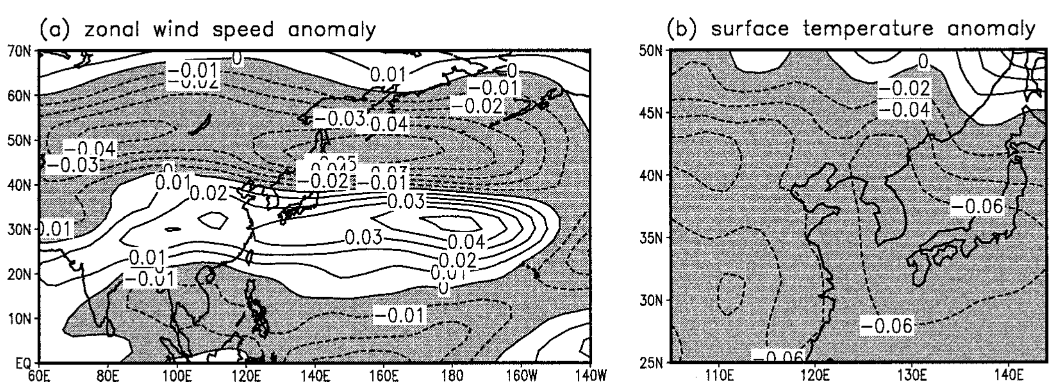

FIG. 3. The structure of the first mode (53.95%) of SVD between the anomalous surface temperature field and the anomalous zonal wind speed field at 300 hPa. (a) The zonal wind speed anomaly at 300 hPa and (b) the surface temperature anomaly.

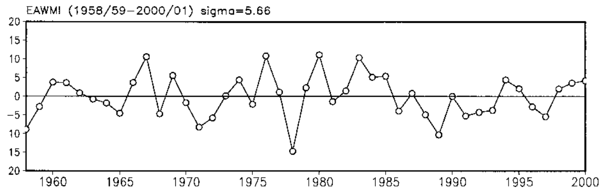

FIG. 5. The time series of the EAWMI from the winter of 1958 to the winter of 2000.

80°–120°E, and is used in the process of defining the EAWMI later, is boxed in Fig. 1a. The wind field at 850 hPa (Fig. 1c) shows that there are two distinct wind direction regimes over East Asia in the northern winter. One is the northwesterly regime north of 20°N, especially over northeastern Asia and the other the easterly regime south of 20°N. Our study is focused only on the former regime. These northwesterlies over northeastern Asia originate from the anticyclonic flow associated with the Siberian high and the cyclonic flow associated with the Aleutian low. They bring the cold air from the polar region into the East Asian region in the northern wintertime. The core of the polar jet stream at the 300-hPa level is evident just south of Japan (Fig. 1e). The position of the jet core is closely related to the meridional temperature gradient at the surface (Fig. 1b) with the thermal wind relationship. As the northwesterly winter monsoon flow over northeastern Asia becomes strong, it brings more cold air and produces a stronger meridional temperature gradient. Therefore, the stronger monsoon flow leads to a stronger polar jet stream over the East Asian region.

Figure 2 shows the correlation coefficient between the SLP averaged over the central area of the Siberian high (boxed region in Fig. 1a) and the zonal wind speed at each grid point at the 300-hPa level. The maximum negative correlation is located in the north of the Korean peninsula with a zonally elongated shape, while the maximum positive correlation is in the region including South Korea and the southern part of Japan where the polar jet core is located. This correlation pattern implies that the jet stream in its core region becomes strong and the zonal wind speed in the maximum negative correlation region becomes weak when the Siberian high develops. In this situation the anomalous cyclonic vorticity over the East Asian region is enhanced and it leads to the development of a trough in the upper level (Eagleman 1985; Holton 1992). This development of a trough is usually associated with the cold surge in the East Asian region.

In order to support the view that the correlation pattern between the Siberian high and the zonal wind speed at 300 hPa is a dynamically significant one, we performed singular value decomposition (SVD) analyses between the surface temperature field over East Asia and other meteorological fields [SLP, the wind vector at 850 hPa (V_{850}), the geopotential height at 500 hPa (Z_{500}), and the zonal wind at 300 hPa (U_{300})] over an area wider than East Asia. Figure 3 shows the structure of the first mode (53.95%) of the SVD between the anomalous surface temperature and the anomalous zonal wind speed field at 300 hPa. The first mode of the SVD between the surface temperature field over the (25°–50°N, 105°–145°E) region (Fig. 3b) and the zonal wind speed field at 300 hPa over the (0°–70°N, 60°E–140°W) region (Fig. 3a) is the most significant case. Figure 3 illustrates clearly the good relationship between the anomalous surface temperature field and the anomalous zonal wind speed field in the region concerned and shows a pattern very similar to Fig. 2.

Therefore, it is reasonable to use the zonal wind speeds averaged over the boxed regions of Fig. 2 to define the EAWMI. The EAWMI is defined as the difference in the area-averaged zonal wind speed at the 300-hPa level between the two boxed regions. That is,

$$\mathrm{EAWMI} = U_{300}(27.5°\text{–}37.5°\mathrm{N},\ 110°\text{–}170°\mathrm{E}) - U_{300}(50°\text{–}60°\mathrm{N},\ 80°\text{–}140°\mathrm{E}).$$

This index is not very sensitive to the boxed area of the negative correlation coefficient. The correlation coefficient between the EAWMI and the first SVD mode of U_{300} (Fig. 3a) is 0.88 (99% significance level).

The correlation pattern between the EAWMI and the surface temperature at each grid point is shown in Fig. 4. The highly negatively correlated area of more than 95% significance covers the East Asian region, in which the highest correlation coefficient of −0.8 falls on the southern part of the Korean peninsula and the middle part of Japan. This figure suggests that the decrease (increase) in surface temperature in the East Asian region is large when the EAWMI is large and positive (negative). This is physically understandable in the following way. As the Siberian high develops, the northwesterly flow and thus the cold advection becomes strong in the East Asian region and leads to the strengthening of the meridional temperature gradient just south of Korea and Japan. The strong meridional temperature gradient is associated with the strong jet stream in the jet core region. The anomalous cyclonic vorticity to the north of the jet stream enhances the anomalous cyclonic circulation and monsoon trough at 500 hPa over the East Asian region. The surface temperature in the East Asian region decreases significantly due to the strong cold advection by strong northwesterlies associated with an enhanced monsoon trough when the EAWMI is large. There is positive feedback between jet stream and surface temperature. Therefore, the EAWMI is a good indicator representing the intensity of the winter monsoon in East Asia, especially in Korea, Japan, and northeastern China.

The correlation pattern between the surface temperature and a winter monsoon index directly obtained by using the mean surface temperature over the region (20°–45°N, 105°–145°E) is very similar to that between the surface temperature and the EAWMI. Therefore, the

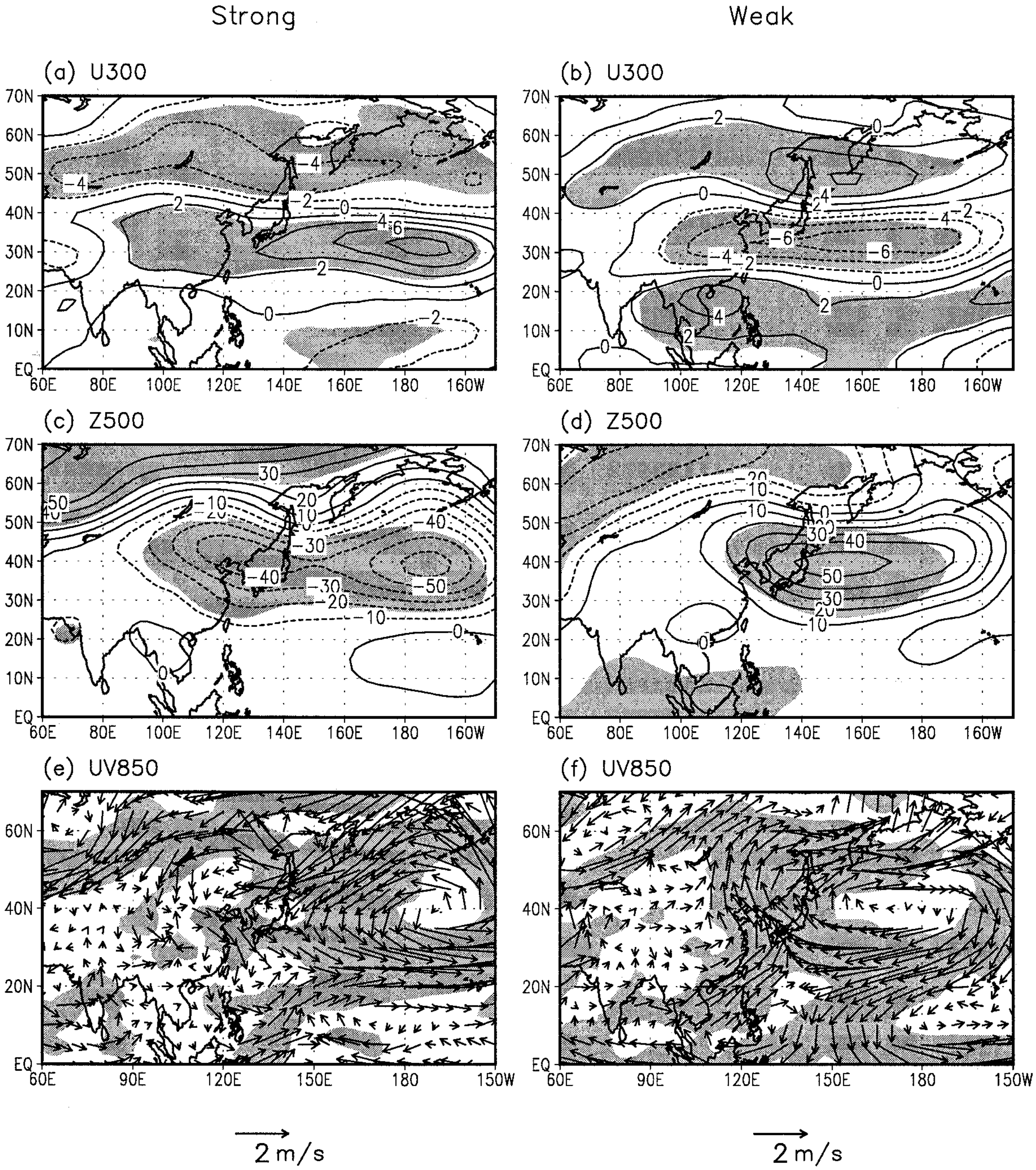

FIG. 6. The composite maps of (a), (b) the zonal wind speed anomaly at 300 hPa; (c), (d) the geopotential height anomaly at 500 hPa; (e), (f) the wind vector anomaly at 850 hPa; (g), (h) the sea level pressure anomaly; and (i), (j) the surface air temperature for strong monsoon winters (left panels) and weak monsoon winters (right panels). The areas exceeding the 95% significance level are shaded.

EAWMI is appropriate for representing climatic features at the surface. The SLP itself averaged over the boxed area in Fig. 1a has been tested as to whether it is a good index to represent the intensity of the winter monsoon in East Asia. The result was that the correlation coefficients between the SLP of the Siberian high region and the surface temperature over East Asia are in general smaller than those between the EAWMI and the surface temperature (not shown). That is, the SLP of the Siberian high region is not as good as the zonal wind speed difference at the 300-hPa level as a winter monsoon index in the East Asian region. The winter monsoon in East Asia is associated with the zonal pressure gradient, which depends strongly on the development of both the Siberian high and Aleutian low. Unlike the index obtained by considering only the variation of the

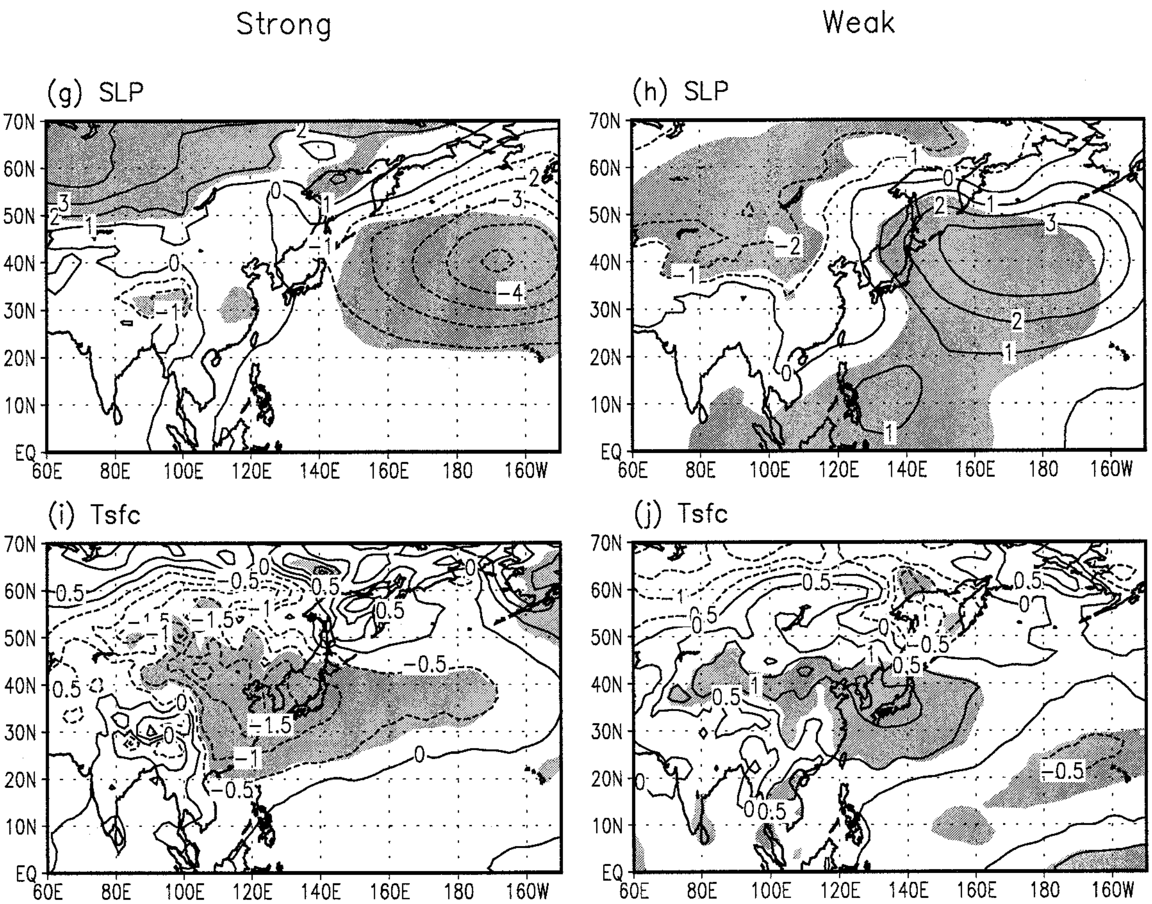

FIG. 6. (*Continued*)

Siberian high SLP, the EAWMI has a good correlation with the variability of the Aleutian low as well as the Siberian high. It should be remembered that the strong winter monsoon in East Asia is closely related to the development of not only the Siberian high but also the Aleutian low.

b. Strong and weak monsoon composites

The time series of the EAWMI from the winter of 1958 to the winter of 2000 yields seven strong winter monsoon years and seven weak winter monsoon years (Fig. 5), based on the 0.9 standard deviation of the index. Here, the winter of 1958 denotes December of 1958, January of 1959, and February of 1959. The seven strong winter monsoon years are 1967, 1969, 1976, 1980, 1983, 1984, and 1985, while the seven weak win-

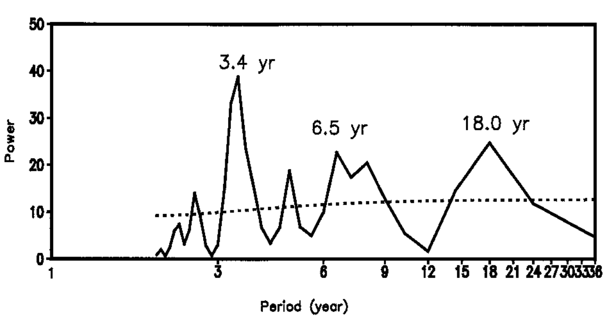

FIG. 7. The power spectrum result for the EAWMI.

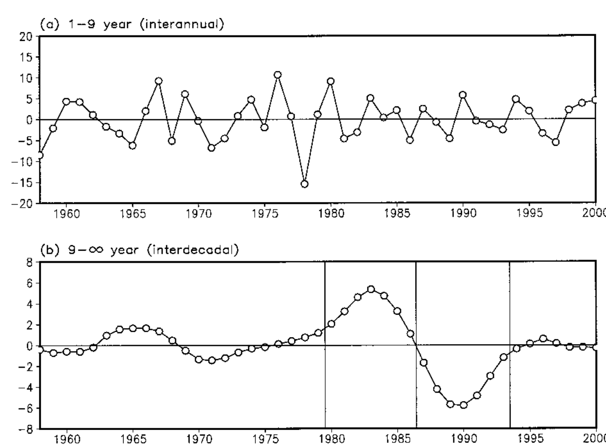

FIG. 8. The time series of the EAWMI for (a) the interannual component and (b) the interdecadal component.

ter monsoon years are 1958, 1971, 1972, 1978, 1989, 1991, and 1997. Among the seven strong monsoon years, 1969 and 1976 are El Niño years and 1984 is a La Niña year but the others are normal years. On the other hand, 1971 is a La Niña year, 1972, 1991 and 1997 are El Niño years, and the others are normal years among the seven weak monsoon years. Therefore, the winter monsoon variation in the East Asian region does not seem to be closely related to ENSO phenomena. However, there is a tendency that El Niños occur in much more negative EAWMI years than positive EAWMI years. It is reversed for La Niñas (Fig. 5). Also, the south East Asian regions, such as the southeast part of China, the southeast China Sea, and the western North Pacific, have some meaningful correlations with ENSO, as was previously mentioned in the introduction (Zhang et al. 1996, 1997; Wang et al. 2000).

The composite maps of anomalies of the meteorological variables for strong monsoon winters and weak monsoon winters are shown in Fig. 6. All anomaly patterns in strong monsoon winters are clearly contrasted with those in weak monsoon winters. The strong monsoon winters are characterized by the strengthened polar jet stream at the 300-hPa level, the deepened Aleutian low at the 500-hPa level and the surface, the strengthened northerly winds at the 850-hPa level in the East Asian region especially along the Russian coast, the developed Siberian high, and the cooler surface temperatures in East Asia. Most of the anomalies are significant at the 95% level of a Student's *t* test (shaded area in Fig. 6) in the central areas of the anomaly. It is worthy of note that most anomaly patterns in the weak monsoon winters are opposite to those in the strong monsoon winters even in the remote areas, as well as in the East Asian region (not shown for the global pattern). This implies that the East Asian winter monsoon system is linked to the global circulation.

c. Interannual and interdecadal components

The dominant periods embedded in the EAWMI are shown in Fig. 7. The predominant peaks in the EAWMI are at 3.4, 18.0, and 6.5 yr. The EAWMI has a strong interdecadal variability as well as a strong interannual variability. Thus, the period of the EAWMI can be divided into two components: the interannual component and the interdecadal component.

Figure 8 shows the time series of the EAWMI for the interannual component (period of 1–9 yr) and the interdecadal component (period of more than 10 yr). It is noted that the EAWMI is dominated by the interannual component before 1980 and by both the interannual and interdecadal components from 1980 to 1993. In other words, the time series of the interannual component of the EAWMI (Fig. 8a) is almost the same as that of the EAWMI itself (Fig. 5) before 1980 but the time series of the interdecadal component of the EAWMI (Fig. 8b) shows the opposite phase of the EAWMI to be dominant from 1980 to 1993. If one projects the meteorological anomaly fields onto the time series of either the EAWMI or its interannual/interdecadal component, those regressed fields can be obtained. Regressed field patterns of meteorological elements such as U_{300}, Z_{500}, U_{750}, V_{850}, T_{sfc}, and SLP for the original value of the EAWMI and its interannual component are similar to their composite patterns for strong monsoons (not shown). Those patterns of SLP, Z_{500}, and U_{300} for the interannual and interdecadal components are shown in Fig. 9. The right panel of Fig. 9 illustrates that the interdecadal component is the negative phase of the Arctic Oscillation (AO). Figure 10 shows the second and the first EOFs of SLP and the regressed fields of each mode. The first EOF mode of SLP is called AO, and the SLP pattern and the regressed fields of the first mode (Fig. 10, right panels) are very similar to the interdecadal component of the East Asian winter monsoon. This implies that the East-Asian winter monsoon system is associated with AO on an interdecadal time scale. On the other hand, the interannual component (Fig. 9, left panels) has a very similar pattern to the second mode of the EOF of SLP and its associated regressed field (Fig. 10, left panels).

The anomaly fields in seven strong monsoon winters (1980–86), which are indicated by vertical dashed lines in Fig. 8b, are compared to those in seven weak monsoon winters (1987–93) in Fig. 11. The anomaly patterns of zonal wind speed at 300 hPa are clearly contrasted in the distribution of opposite signs between strong and weak monsoon winters. Other patterns of variables such as geopotential heights at 500 hPa, wind vectors at 850 hPa, and surface temperatures also have contrasting features like the zonal wind speed at 300 hPa (not shown). However, no distributions of opposite sign between strong and weak monsoon winters exist in the whole pattern of sea level pressure. That is, the AO pattern of positive phase is clear in the weak monsoon period, while that of negative phase is not clear in the strong monsoon period (Figs. 11b and 11d). If we choose the strong and weak monsoon periods with a 10-yr interval, that is, 1976–85 for the strong monsoon winter and 1988–97 for the weak monsoon winter, we can see the obvious opposite patterns between these two periods even in the distribution of sea level pressure anomalies (not shown). This implies that AO occurs more clearly in the regressed fields on the decadal time scale rather than on the interannual time scale.

We mentioned the necessity of the separation of the interannual and the interdecadal monsoon variabilities in East Asia in the introduction. From considering the interannual and interdecadal components, we find that the climate patterns associated with the two components are different from each other and that one of the dynamics controlling the interdecadal component may be AO.

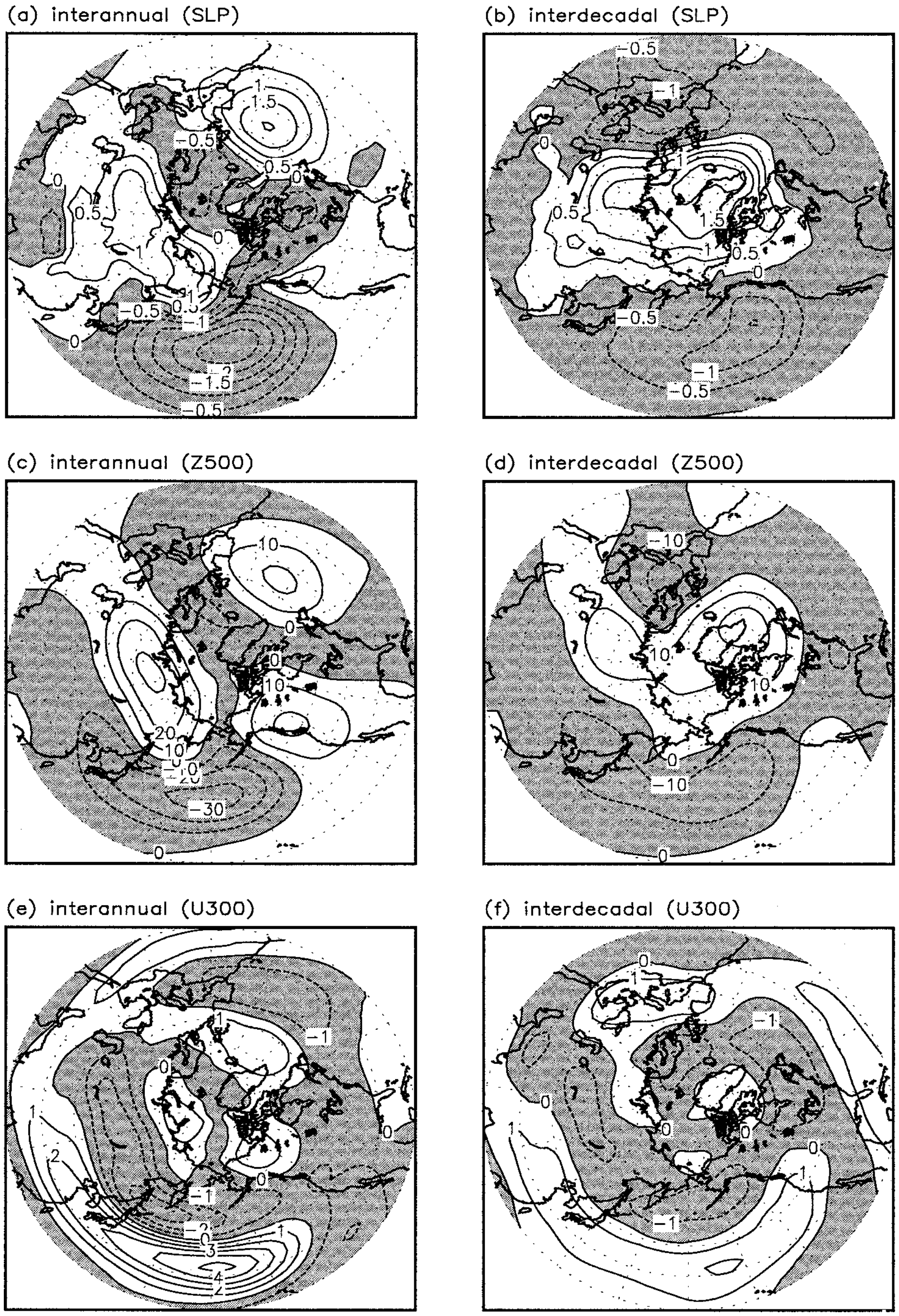

FIG. 9. The regressed fields of (a), (b) sea level pressure; (c), (d) geopotential height at 500 hPa; and (e), (f) zonal wind speed at 300 hPa for the interannual component (left panels) and the interdecadal component (right panels).

4. Effects of snow cover in autumn on the East Asian winter monsoon

One of the possible factors affecting the East Asian winter monsoon system is the snow cover over the Siberian high region. The variation of snow cover in autumn over this region is positively correlated with the EAWMI (Fig. 12). This implies that a strong winter monsoon is expected when the snow cover is large in autumn. Figure 12 shows another area where the correlation coefficient is relatively high, that is, northeastern China and far eastern Russia. Clark and Serreze (2000) revealed that the snow cover in winter over these

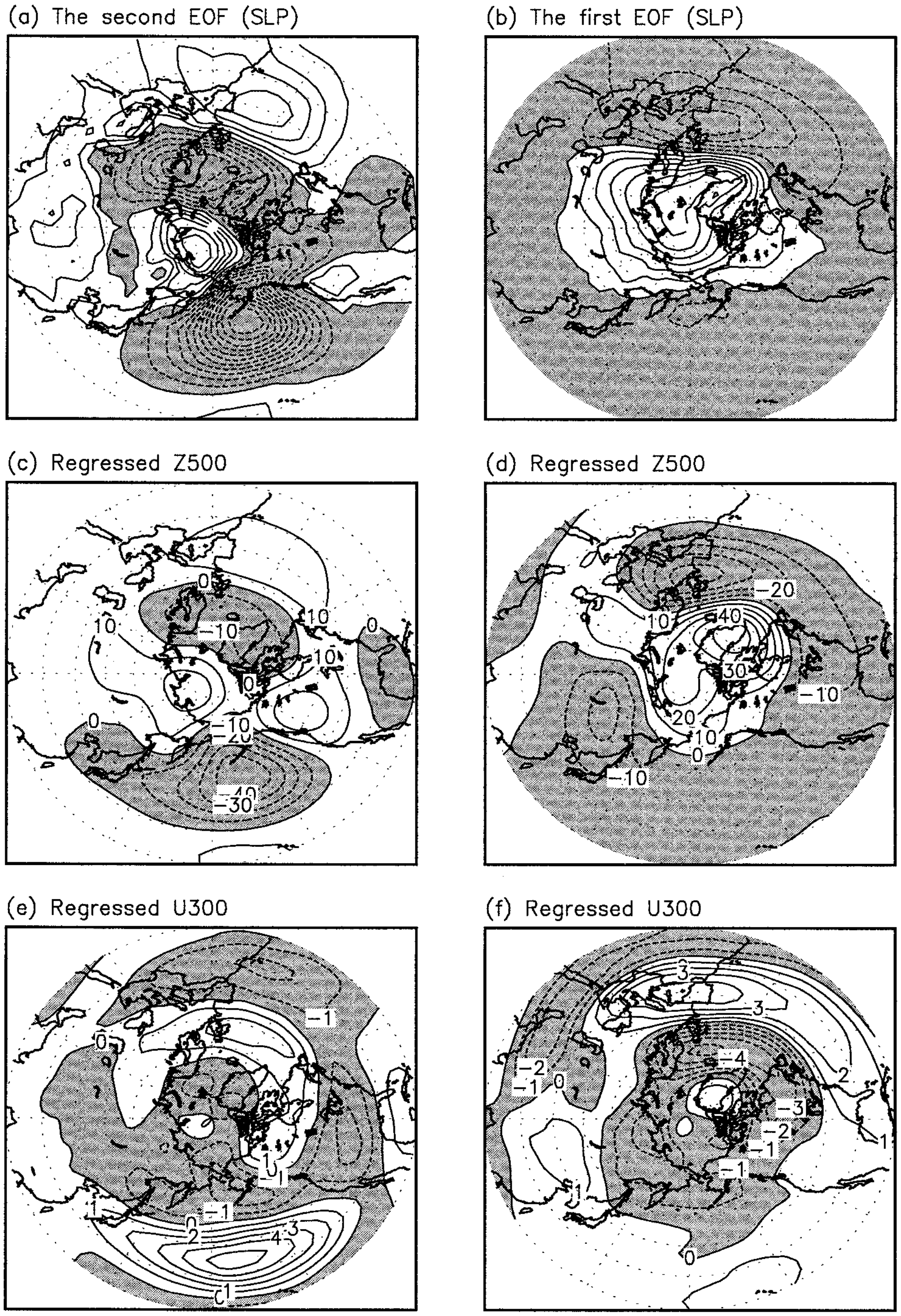

FIG. 10. The EOF modes of (a), (b) the sea level pressure; (c), (d) the regressed fields of the geopotential height at 500 hPa; and (c), (f) the zonal wind speed at 300 hPa for the second mode (left panels) and the first mode (right panels).

areas is closely associated with the atmospheric circulation over the North Pacific Ocean during the boreal winter. According to their result the Aleutian low is deepened when the anomaly of snow cover north of the Korean peninsula is positively large. The pattern of the EAWMI–snow cover correlation for only October is very similar to Fig. 12 with a stronger correlation, but the correlation for September or November is more or less insignificant (not shown). The reason for the increased correlation in October is that there is little snow in September while the snow already covers a large area in November.

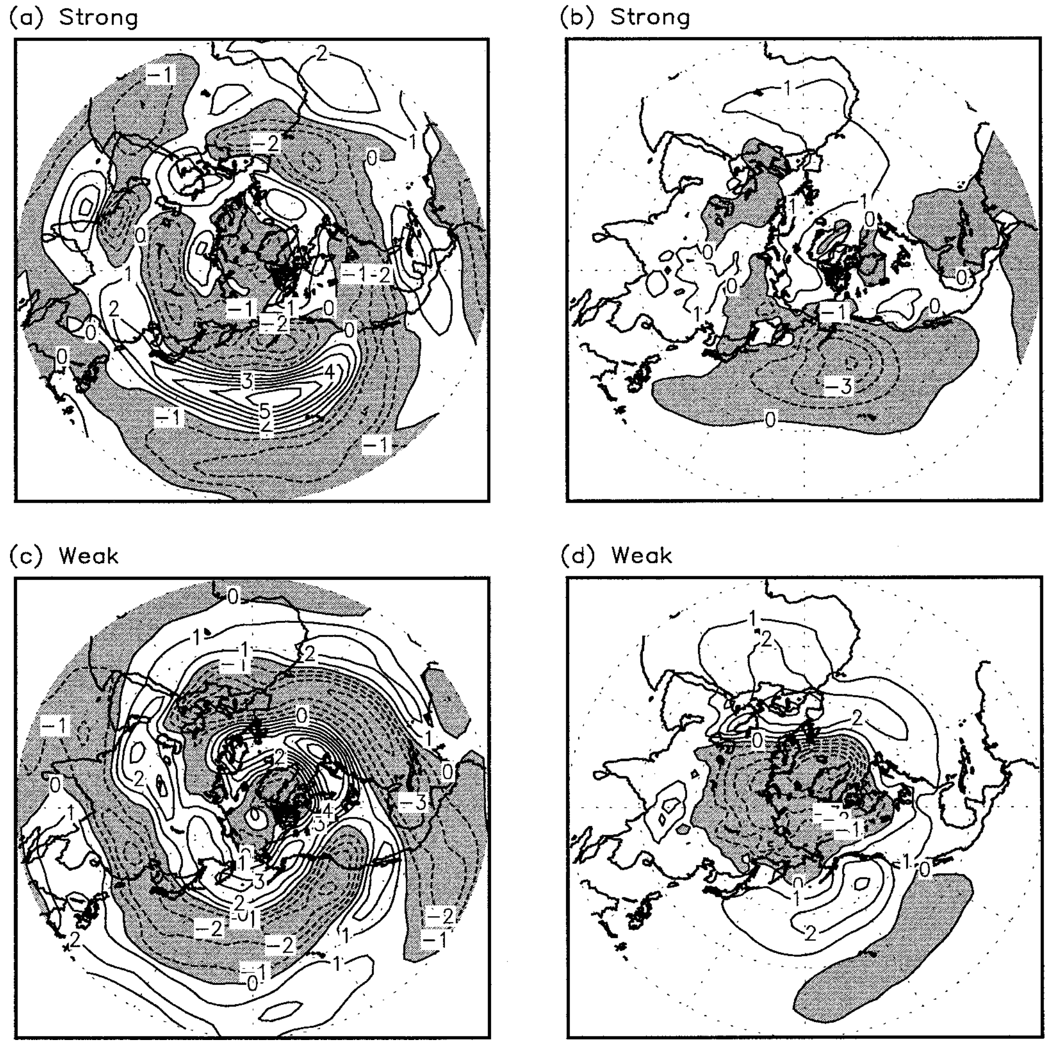

Fig. 11. The anomaly fields of (a), (c) the zonal wind speed at 300 hPa and (b), (d) the sea level pressure for the strong monsoon winters of 1980–86 (top panels) and the weak monsoon winters of 1987–93 (bottom panels).

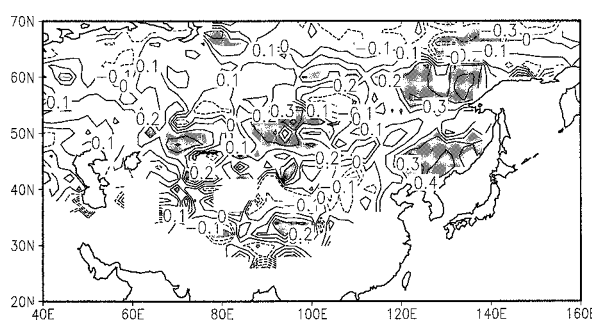

Fig. 12. The correlation coefficients between the snow cover in autumn and the EAWMI. The areas exceeding the 95% significance level are shaded.

The differences in the snow cover anomaly in autumn and winter between the weak monsoon period and the strong monsoon period are shown in Fig. 13. It is evident that the snow cover over the Siberian high region in the weak monsoon period (1987/88–1993/94) is much less than that in the strong monsoon period (1980/81–1986/87). This is more dominant in autumn than in winter. This result supports Fig. 12. It suggests that a strong winter monsoon is anticipated when a strong positive snow cover anomaly over the Siberian high region and the region north of the Korean peninsula exists in autumn. In order to confirm the effect of the snow cover anomaly in autumn, some model experiments have been performed. The previous observational and model results (Walsh and Ross 1988; Walland and Simmonds 1997; Clark and Serreze 2000) show the simultaneous correlation between snow cover and the circulation in winter. In this paper, we focus on the lag correlation between snow cover in autumn and the circulation in winter.

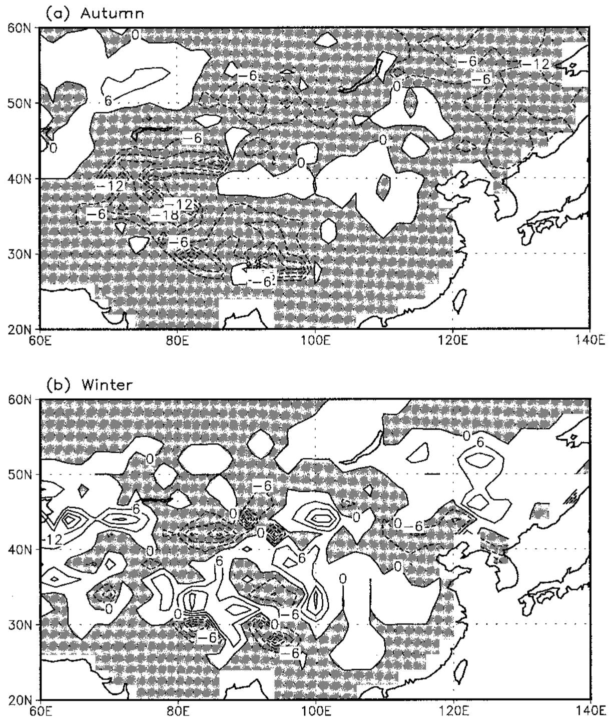

FIG. 13. The snow cover difference (weak monsoon period minus strong monsoon period) in (a) autumn and (b) winter.

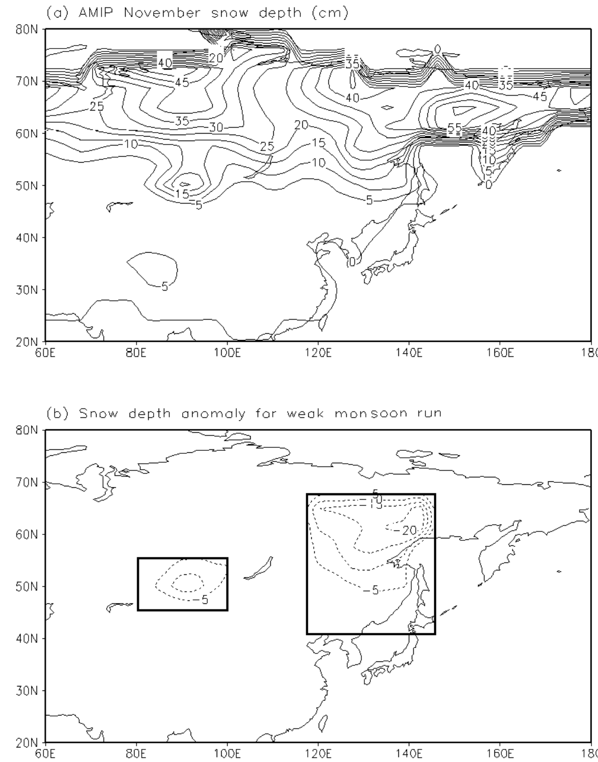

FIG. 14. The initial conditions of (a) the snow depth for the control run and (b) the snow depth anomaly for the weak monsoon runs.

The model used in our study is the SNU-AGCM. For a description of the model, the reader is referred to Lee et al. (2002) and Kim (1999). The snow depth has been used in our model experiments instead of the snow cover, because the SNU-AGCM cannot handle the snow cover. For weak monsoon runs the initial condition has been taken as half of the snow depth over both the Siberian high region and the region north of the Korean peninsula (Fig. 14b). The model integration has been performed from 1 November to 28 February. The control run has been done using the AMIP November snow depth (Fig. 14a) and five ensemble runs have been performed with different atmospheric situations. The results for the northern midwinter are shown in Fig. 15. The weakening of the polar jet stream at 300 hPa, the filling of the Aleutian low, and the warming of the surface temperature over the Siberian high region are predominant, although the centers of the anomalies have been shifted eastward. Since the sea level pressure and geopotential height at 500 hPa show the AO pattern, we can expect that the interdecadal variation associated with the East Asian monsoon (right panels of Fig. 9 and Fig. 10) may be influenced by the variation in the snow cover in autumn. By observational analysis, Watanabe and Nitta (1999) showed that the decrease of the snow cover over East Asia in autumn results in an AO-like pattern: the increase of the surface temperature in East Asia, the decrease of the sea level pressure and geopotential height at 500 hPa in the Arctic region, and the increase of the sea level pressure and geopotential height at 500 hPa in the North Pacific. Thus, by an enhanced AO pattern on the decadal time scale, the amount of snow over the above-mentioned area in autumn could certainly be one of the factors affecting the decadal variation of the East Asian winter monsoon.

5. Teleconnections

In order to investigate the possibility of a remote connection, the EAWMI defined in our paper is compared to other indices such as the North Pacific index (NP), the North Atlantic Oscillation index (NAO), the Arctic Oscillation index (AO), Niño-3.4, the Siberian high index (SH), and the Pacific decadal oscillation (PDO) index. The NP defined by Trenberth and Hurrell (1994) is the sea level pressure anomaly averaged over the region between 30°–65°N and 160°E–140°W. This index represents well the Aleutian low variation. The NAO has been defined by Hurrell (1995) as

$$\mathrm{NAO} = 0.5 \times [P'(40°\mathrm{N}, 10°\mathrm{W}) - P'(65°\mathrm{N}, 20°\mathrm{W})],$$

where P' is the SLP anomaly. The AO and the PDO denote the time series of the first EOF mode of SLP and the North Pacific SST, respectively. On the other hand, the Niño-3.4 index is defined as the SST anomaly averaged over the region between 5°S–5°N and 170°E–120°W, and SH is defined as the SLP anomaly averaged over the area between 40°–60°N and 80°–120°E.

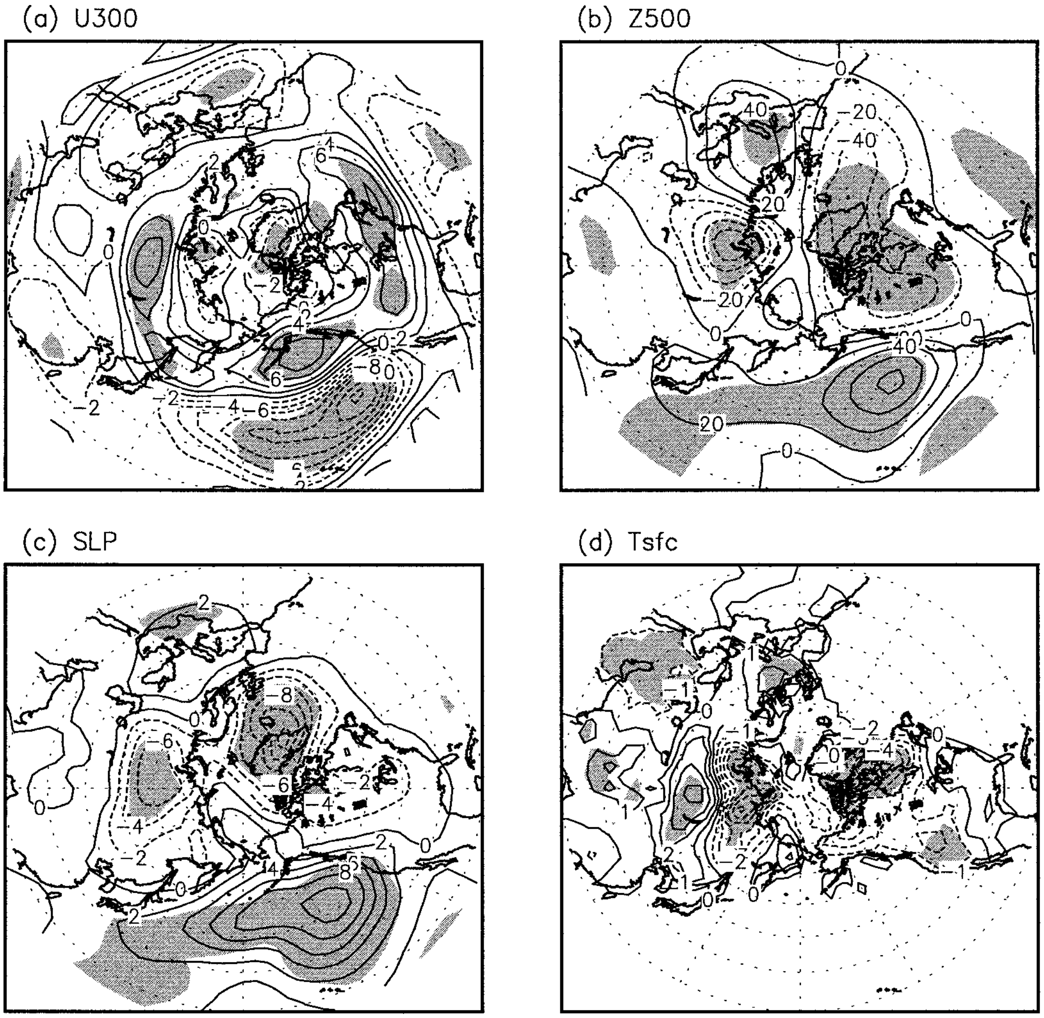

FIG. 15. The model results for Jan from five ensemble runs in the case of a weak winter monsoon. The areas exceeding the 95% significance level are shaded.

The correlation coefficients between the EAWMI and various indices for the unfiltered data, and the interannual component and the interdecadal component are summarized in Tables 1–3, respectively. The correlation coefficients between NP–SH and the EAWMI using unfiltered data, and the interannual and interdecadal components are all high. For NAO, AO, and PDO, the correlation coefficients with the EAWMI using the interdecadal component are much higher than those using unfiltered data and the interannual component. By contrast, the correlation coefficient between Niño-3.4 and the EAWMI for the interannual component is the most significant among the three correlation coefficients. For the interannual component, the EAWMI has a significant negative correlation (−0.48) with NP and a positive correlation (0.68) with SH as expected. However, other indices have little correlation with the EAWMI. The anticorrelation between NP and Niño-3.4 shown in Ta-

TABLE 1. Correlation coefficients between the EAWMI and various indices for the unfiltered data.

	EAWMI	NP	NAO	AO	Niño-3.4	SH
NP	−0.50*	1.00				
NAO	0.03	0.01	1.00			
AO	−0.16	0.17	0.77*	1.00		
Niño-3.4	−0.21	−0.39*	−0.03	−0.07	1.00	
SH	0.61*	−0.30*	−0.24	−0.30	−0.09	1.00
PDO	0.05	−0.02	0.20	0.18	0.02	−0.05

* Significant at 95% level.

TABLE 2. Same as in Table 1 except for the interannual component.

	EAWMI	NP	NAO	AO	Niño-3.4	SH
NP	−0.48*	1.00				
NAO	0.24	0.06	1.00			
AO	0.05	0.15	0.69*	1.00		
Niño-3.4	−0.25	−0.45*	−0.10	−0.16	1.00	
SH	0.68*	−0.25	0.11	−0.06	−0.17	1.00
PDO	0.23	−0.04	0.03	0.02	−0.15	0.14

* Significant at 95% level.

ble 2 is well known, and is associated with the Pacific–North American (PNA) pattern over this area. On the other hand, for the interdecadal component, the correlation between the EAWMI and NAO–AO is strong and negative. (Note that there is little correlation between the EAWMI and NAO–AO for the interannual component.) This implies that AO or NAO is closely associated with the East Asian winter monsoon system on the decadal time scale. Another interesting feature of the teleconnection for the interdecadal component is that AO or NAO has a strong negative correlation with SH. However, AO and NAO have no correlation with NP on the decadal time scale. Therefore, AO or NAO may affect the Siberian high but not the Aleutian low and thus ultimately influence the East Asian winter monsoon system on the decadal time scale.

Previous studies support our results about the relationship between AO–NAO and the East Asian winter monsoon. Thompson and Wallace (2001) showed that cold events occur with much greater frequency over East Asia under low-index AO conditions. Gong et al. (2001) also revealed that the wintertime temperature over eastern China is strongly connected to SLP variation at high latitudes on the Eurasian continent (the Siberian high region), and the negative phase of AO is associated with the strong Siberian high. Therefore, the negative phase of AO is related to the cold winter in eastern China. In this paper, we have suggested that the relationship among AO–NAO, the Siberian high, and the East Asian winter monsoon is dominant on the interdecadal time scale and not on the interannual time scale. The relation between AO–NAO and the Siberian high may be explained by the temperature advection from high latitude associated with AO–NAO (Thompson and Wallace 2000a).

6. Summary

Most study on the East Asian monsoon has been performed in relation to the northern summer features, which are associated with precipitation. The northern winter monsoon, which is mainly associated with temperature, has been given relatively less attention than the summer monsoon. The region that covers Korea, Japan, and the northeastern part of China experiences cold or warm winters depending on the intensity of the East Asian monsoon. The surface temperature in this region strongly depends on the cold advection due to the prevailing northwesterlies. In order to describe the intensity of the winter monsoon over this area, an appropriate index is necessary. A new East Asian winter monsoon index (EAWMI) defined in our study is very good for representing the winter monsoon over the northeastern part of Asia, especially for Korea, Japan, and northeastern China.

The composite maps for strong winter monsoons and weak winter monsoons using our monsoon index show distinct opposite patterns in the meteorological variables, such as the zonal wind at 300 hPa, the geopotential height at 500 hPa, the wind vector at 850 hPa, the sea level pressure, and the surface temperature, in the middle and high latitudes of the Northern Hemisphere. These maps for strong monsoons indicate (i) the enhanced polar jet stream at 300 hPa, (ii) the strengthened trough in the East Asian region and the developed Aleutian low at 500 hPa, (iii) the increased northerly wind speeds at 850 hPa along the Russian coast, and (iv) the developed Siberian high and Aleutian low at the surface.

From the power spectrum analysis of the EAWMI, the EAWMI could be divided into two components: the

TABLE 3. Same as in Table 1 except for the interdecadal component.

	EAWMI	NP	NAO	AO	Niño-3.4	SH
NP	−0.54*	1.00				
NAO	−0.51*	0.09	1.00			
AO	−0.68*	0.08	0.87*	1.00		
Niño-3.4	0.00	−0.20	0.19	0.24	1.00	
SH	0.55*	−0.41*	−0.73*	−0.59*	0.07	1.00
PDO	−0.43*	0.04	0.52*	0.55*	0.52*	−0.32

* Significant at 95% level.

interannual component and the interdecadal component. The regressed fields from the projection onto the interannual components of the EAWMI resemble the second EOF of SLP and the related regressed fields. The regressed field patterns for the interdecadal component are not similar to those for the interannual one, but indicate an Arctic Oscillation. This implies that the East Asian winter monsoon system is associated with the Arctic Oscillation index (AO) on the decadal time scale.

The snow cover/snow depth in autumn can be one of the factors influencing the intensity of the East Asian winter monsoon. The variation of snow cover in autumn, especially in October, over the Siberian high region and the region of northeastern China and far eastern Russia is positively correlated with the EAWMI. This suggests that a strong (weak) winter monsoon is expected when the snow cover over the above-mentioned region is large (small) in autumn. The results of our model experiments using the snow depth data support this observational analysis and show an AO-like pattern and the close relationship between the variation of the Aleutian low and the snow amount in the East Asian region. Therefore, it can be expected that the snow cover in autumn over the Siberian high region and the region of northeastern China and far eastern Russia is associated with the decadal variation of the East Asian winter monsoon.

The EAWMI has been compared to other indices such as the North Pacific index (NP), the North Atlantic Oscillation index (NAO), the AO, the Niño-3.4 region, the Siberian high index (SH), and the Pacific decadal oscillation (PDO). The interannual component of the EAWMI is negatively correlated with NP and positively correlated with SH. On the other hand, the interdecadal component of the EAWMI has a negative correlation with NP, NAO, and AO, and is positively correlated with SH. It is noted that the EAWMI is strongly associated with NAO or AO on the decadal time scale only. Furthermore, NAO or AO is strongly negatively correlated with SH on this time scale only. This fact implies that the East Asian winter monsoon system may be associated with the Arctic Oscillation through the Siberian high on the decadal time scale.

7. Discussion

The different patterns of interannual and interdecadal variabilities of the East Asian winter monsoon may be controlled by different factors. For the interannual variability, the East Asian winter monsoon is controlled by the interannual variation of the Siberian high and the Aleutian low. The possible factors that affect the interannual variability of the Siberian high are the local Hadley circulation caused by convection in the western Pacific (Zhang et al. 1997), the interannual variability of radiative cooling (Ding and Krishnamurti 1987), the Tibetan Plateau (Murakami 1987), and so on. On the other hand, one of the possible factors that influence the interannual variability of the Aleutian low is ENSO.

For the interdecadal variability, we expect that the interdecadal variation associated with the East Asian monsoon may be controlled by the variation of snow cover/snow depth in autumn, since the sea level pressure and the geopotential height at 500 hPa for responses to the snow cover/snow depth in autumn in our model experiments show an AO-like pattern. Watanabe and Nitta (1999) indicated that the snow cover over the Eurasian continent in autumn is associated with an AO-like pattern in the atmospheric circulation in winter. However, the snow cover anomalies in autumn were like pulses, with a decadal time scale, in contrast to the continuous anomalies in the atmosphere. The snow cover/snow depth is thought to be an internal variable of climate. Therefore, it is likely that the snow anomalies in autumn in eastern Eurasia may have a role as an amplifier for the atmospheric shifts. From the relationship between the EAWMI and the climate indices, the snow cover over the Siberian high region, northeastern China, and far eastern Russia in autumn may be associated with the interdecadal variation of AO in winter, and then the interdecadal variation of AO influences the interdecadal variation of the Siberian high and the East Asian winter monsoon.

The mechanism that is linking the snowfall in autumn to the decadal variability of the winter monsoon intensity could be explained as follows. The decrease of snow cover/snow depth over East Asia in autumn assists the increase in surface temperature and upward motion over the same region. The integration of our model shows that the warm surface region extends eastward, the region of upward motion also shifts eastward, and the upward motion strengthens (not shown). This upward motion induces a compensating downward motion and the associated convergence field is also enhanced in the upper layer over the North Pacific. Therefore, the decrease of snow cover/snow depth in autumn over East Asia could lead to a weakening of the Aleutian low. On the other hand, a lack of autumn snow cover would lead directly to a delay and weakening of the buildup of cold air over the Siberian high region by the weak cold advection from high latitudes associated with a positive phase of AO. Through this procedure, the reduced snowfall in autumn over the Siberian high region, the region of northeastern China, and far eastern Russia induces the weak East Asian winter monsoon.

Our new winter monsoon index is an alternative tool for describing the winter monsoon system in the East Asia region quantitatively, especially in Korea, Japan, and the northeastern part of China, while in previous studies, most monsoon indices described the monsoon system in the southeastern part of China. Our index, EAWMI, well described the characteristics of the East Asian winter monsoon, and could be easily used to reveal the relationship between the winter monsoon and global climate variability. Using this index, we could also show the interannual and interdecadal variations of the winter monsoon, which have not been considered up to now. We hope that our new index will be widely used to reveal unexplained monsoon features and their associated mechanisms in the near future.

Acknowledgments. This research was performed for the project Development of Forecast Techniques for the East Asian Monsoon–Changma Circulation System, one of the Meteorological and Earthquake Research and Development programs funded by the Korea Meteorological Administration (KMA). The authors would like to thank Dr. Wang and Dr. An (IPRC, Honolulu, Hawaii) for their helpful suggestions, and also the two anonymous reviewers for their valuable comments.

REFERENCES

Chang, C.-P., and K.-M. Lau, 1982: Short-term planetary-scale interaction over the tropics and the midlatitudes during northern winter. Part I: Contrast between active and inactive periods. *Mon. Wea. Rev.,* **110,** 933–946.

——, J. Erickson, and K.-M. Lau, 1979: Northeasterly cold surges and near-equatorial disturbances over the winter-MONEX area during 1974. Part I: Synoptic aspects. *Mon. Wea. Rev.,* **107,** 812–829.

Clark, M. P., and M. C. Serreze, 2000: Effects of variations in East Asian snow cover on modulating atmospheric circulation over the North Pacific Ocean. *J. Climate,* **13,** 3700–3710.

Ding, Y. H., 1990: Buildup, air-mass transformation and propagating of Siberian high and its relations to cold surge in East Asia. *Meteor. Atmos. Phys.,* **44,** 281–292.

——, and T. N. Krishnamurti, 1987: Heat budget of the Siberian high and the winter monsoon. *Mon. Wea. Rev.,* **115,** 2428–2449.

Eagleman, J. R., 1985: *Meteorology.* 2d ed. Wadsworth Publishing, 394 pp.

Gong, D.-Y., S.-W. Wang, and J.-H. Zhu, 2001: East Asian winter monsoon and Arctic oscillation. *Geophys. Res. Lett.,* **28,** 2073–2076.

Holton, J. R., 1992: *An Introduction to Dynamic Meteorology.* 3d ed. Academic Press, 511 pp.

Hurrell, J. W., 1995: Decadal trends in the North Atlantic Oscillation: Regional temperatures and precipitation. *Science,* **269,** 676–679.

Kalnay, E., and Coauthors, 1996: The NCEP/NCAR 40-Year Reanalyses Project. *Bull. Amer. Meteor. Soc.,* **77,** 437–471.

Kerr, R. A., 1999: A new force in high-latitude climate. *Science,* **284,** 241–242.

Kim, J.-K., 1999: Parameterization of land surface processes in an atmospheric general circulation model. Ph.D. thesis, Seoul National University, 178 pp.

Kitoh, A., 1988: Correlation between the surface air temperature over Japan and the global sea surface temperature. *J. Meteor. Soc. Japan,* **66,** 967–986.

Lau, K.-M., K.-M. Kim, and S. Yang, 2000: Dynamical and boundary forcing characteristics of regional components of the Asian summer monsoon. *J. Climate,* **13,** 2461–2482.

Lee, E.-J., J.-G. Jhun, and I.-S. Kang, 2002: The characteristic variability of boreal wintertime atmospheric circulation in El Niño events. *J. Climate,* **15,** 892–904.

Mantua, N. J., S. R. Hare, Y. Zhang, J. M. Wallace, and R. C. Francis, 1997: A Pacific interdecadal climate oscillation with impacts on salmon production. *Bull. Amer. Meteor. Soc.,* **78,** 1069–1079.

Murakami, T., 1987: Effects of the Tibetan Plateau. *Monsoon Meteorology,* C.-P. Chang and T. N. Krishnamurti, Eds., Oxford University Press, 235–270.

Overland, J. E., J. M. Adams, and N. A. Bond, 1999: Decadal variability of the Aleutian low and its relation to high-latitude circulation. *J. Climate,* **12,** 1542–1548.

Thompson, D. W. J., and J. M. Wallace, 2000a: Annular modes in the extratropical circulation. Part I: Month-to-month variability. *J. Climate,* **13,** 1000–1016.

——, and ——, 2000b: Annular modes in the extratropical circulation. Part II: Trends. *J. Climate,* **13,** 1018–1036.

——, and ——, 2001: Regional climate impacts of the Northern Hemisphere annular mode. *Science,* **283,** 85–89.

Trenberth, K. E., and J. W. Hurrell, 1994: Decadal atmosphere–ocean variations in the Pacific. *Climate Dyn.,* **9,** 303–319.

Walland, D. J., and I. Simmonds, 1997: Modeled atmospheric response to changes in Northern Hemisphere snow cover. *Climate Dyn.,* **13,** 25–34.

Walsh, J. E., and B. Ross, 1988: Sensitivity of 30-day dynamical forecasts to snow cover. *J. Climate,* **1,** 739–754.

Wang, B., and Z. Fan, 1999: Choice of south Asian summer monsoon indices. *Bull. Amer. Meteor. Soc.,* **80,** 629–638.

——, R. Wu, and X. Fu, 2000: Pacific–East Asian teleconnection: How does ENSO affect East Asian climate? *J. Climate,* **13,** 1517–1536.

Watanabe, M., and T. Nitta, 1999: Decadal change in the atmospheric circulation and associated surface climate variations in the Northern Hemispheric winter. *J. Climate,* **12,** 494–510.

Webster, P. J., and S. Yang, 1992: Monsoon and ENSO; selectively interactive systems. *Quart. J. Roy. Meteor. Soc.,* **118,** 877–926.

Yamazaki, K., 1989: A study of the impact of soil moisture and surface albedo changes on global climate using the MRI-GCM-I. *J. Meteor. Soc. Japan,* **67,** 123–146.

Zhang, R., A. Sumi, and M. Kimoto, 1996: Impact of El Niño on the East Asian monsoon: A diagnostic study of the '86/87 and '91/92 events. *J. Meteor. Soc. Japan,* **74,** 49–62.

Zhang, Y., K. R. Sperber, and J. S. Boyle, 1997: Climatology and interannual variation of the East Asia winter monsoon: Results from the 1979–95 NCEP–NCAR reanalysis. *Mon. Wea. Rev.,* **125,** 2605–2619.